Available online at www.sciencedirect.com

SciVerse ScienceDirect

Journal of the European Ceramic Society 32 (2012) 2711–2721

www.elsevier.com/locate/jeurceramsoc

Effects of Ca-, Mg- and Si-doping on microstructures of alumina–zirconia composites

K. Biotteau-Deheuvels, L. Zych [a], L. Gremillard *, J. Chevalier

Université de Lyon, INSA-Lyon, MATEIS, UMR CNRS 5510, 20 Av. A. Einstein, 69621 Villeurbanne Cedex, France

Received 5 October 2011; accepted 2 November 2011
Available online 29 November 2011

Abstract

The aim of this work was to obtain zirconia toughened alumina composites with different microstructures, using a simple process (powder mixing and natural sintering). Adjusting the amount of zirconia directly controls the size and localization of zirconia grains and the size of the alumina grains. Doping the composite with CaO, MgO and SiO_2 allows further control of the microstructures. The influence of the thermal treatments is also investigated. The composites exhibit different structures (nano/nano-, micro/nano- and micro-composites) with zirconia and alumina grains as small as 100 and 200 nm, respectively, and with the proportion of intragranular zirconia grains varying between 0% and 90%. Zirconia plays a major role on grain size distributions as compared to CaO and MgO, whose role is almost negligible. The use of SiO_2 leads to micro/nano composites with intragranular zirconia particles. The influence of these different additions is related to adjustments of the grain boundaries mobility.

Keywords: Nanocomposites; Grain boundaries; Slip casting; Inclusions; Grain size

1. Introduction

"Smaller is better" has been the new trend in the last decade in the ceramic community. It may also apply for the realization of zirconia-toughened alumina composites (ZTA). This well-known composite, already commercialized for wide range of applications such as biomedical implants[1] and structural ceramics, is commonly available as a "micro-composite" (submicronic zirconia grains and 2–5 μm grain size alumina matrix). Those composites offer both higher strength and toughness than alumina and lower sensitivity to ageing than zirconia.[2] Together with their proven biocompatibility, this makes those composites the safest for orthopedic implants application. Such composites are often synthesized with second phase additions to stabilize zirconia. For example, CeramTec AG (Plochingen, Germany) commercializes the BIOLOX delta®, an alumina–zirconia composite approximately containing 18.5 vol.% ZrO_2 stabilized by 1.5 vol.% Y_2O_3 and 1.5 vol.% of mixed oxides such as Cr_2O_3 and SrO.[3]

Nevertheless, most zirconia-toughened alumina composite are still prone to a certain extent of ageing (tetragonal to monoclinic surface phase transformation of zirconia grains in the presence of water [4]), mostly those composites containing yttria-stabilized zirconia.[5,6] The presence of yttrium allows low temperature hydrothermal degradation of the composite even though it permits the addition of large amounts of zirconia in ZTA composites. On the other hand, previous results show that using zirconia without any trivalent second phase addition such as yttria enables the process of ageing-free ZTA.[7–9] The concepts of "Nanocomposites" were almost not attempted on alumina–zirconia composites.[10,11] However, in a previous study, ZTA with an alumina matrix in the micrometer range and nano-sized zirconia particles were developed (1.7 vol.% of intra-granular zirconia nano-particles in alumina), leading to specific mechanical properties – in particular concerning wear and fracture resistance.[12,13] Following the classical concepts of 'Nanocomposites' and the widely used nomenclature of Niihara,[14] micro, micro/nano- or nano-composites could be processed and could possess specific resistance to hydrothermal degradation and particular toughening mechanisms. Our global aim is therefore to determine the consequences of microstructure

* Corresponding author.
E-mail address: laurent.gremillard@insa-lyon.fr (L. Gremillard).
[a] Present address: AGH – University of Science and Technology, Faculty of Materials Science and Ceramics, Al. Mickiewicza 30, 30-059 Krakow, Poland.

0955-2219/$ – see front matter © 2011 Elsevier Ltd. All rights reserved.
doi:10.1016/j.jeurceramsoc.2011.11.011

evolution of ZTA composites on their intrinsic properties. More specifically, this article is focused first on obtaining nano-composites with various microstructures using powder mixing and natural sintering, so that our findings can readily be adapted to industrial process.

A potentially effective approach to control the microstructure is to control the grain boundary mobility. One can take inspiration in the work conducted on abnormal grain growth in alumina.[15–18] In particular, the influence of dopants on sintering and grain growth in alumina has been extensively studied: the amount and nature of dopants, as well as the ratio between them when several dopants are used, strongly influence the shrinkage rates during sintering, the final density and the final microstructure. Despite much progress, the mechanisms for abnormal grain growth and the role of magnesia as a sintering aid are still debated since the 1950s. Recently, Dillon and Harmer report that abnormal grain growth (AGG) is diffusion controlled,[19] and explain that a change in interface properties or kinetics may indicate a change in the grain boundary "phase" called a complexion, that produces a characteristic grain boundary transport rate.[20] Ceramics may contain multiple different complexions that are chemically induced by certain additives and could be the root explanation for AGG.[21,22]

With respect to this mechanism, it becomes obvious that grain boundary diffusion coefficient is sensitive to a small amount of cation-doping. To date, two categories of "useful" dopants can be distinguished. On one hand, some dopants favor sintering and decrease grain boundary mobility. Among the most famous, MgO[23–26] enhances densification rate, grain-uniformity and final density of alumina during sintering, but decreases grain growth rate. Magnesia is known to lower the grain boundary mobility in alumina,[24] and more important to favor the presence of only one highly ordered complexion, thus preventing AGG.[20]

On the other hand, the ones that favor anisotropic grain boundary mobility and thus AGG are cited below. SiO_2[27–29] and CaO[30] lead to abnormal grain growth and provoke an increase in the aspect ratio of the grains. Divalent and tetravalent cations in alumina are expected to be compensated by an anion and cation vacancy, respectively, which enhances the diffusivity in alumina. The dopant effect cannot be only explained by the dopant cation ionic valence (MgO and CaO would have the same effect), nevertheless the ionicity is a critical factor to determine the high temperature grain boundary diffusion in polycrystalline alumina.[31]

These previous studies of AGG provide us with tools to improve and control the microstructure of zirconia-toughened alumina composites, in order to process micro-, micro/nano- and nano/nano-composites. Such structures could be obtained by:

- Adjusting the amount of zirconia[32]: indeed, small zirconia particles have a well-known "pinning effect "on alumina grain boundaries.
- Controlling the grain growth with dopants to improve or inhibit the alumina grain growth: highly mobile alumina–alumina grain boundaries may allow the growth of alumina grains around zirconia particles before zirconia particles start to coalesce, leading to intra-type micro/nano composites; dopants used here are CaO and SiO_2. On the other hand, less mobile grain boundaries may possibly lead to nano/nano composites; the potential of MgO to achieve this goal is investigated.
- Adjusting the sintering thermal treatment.

This is therefore the aim of the present work to systematically describe for the first time the effect of zirconia particles and dopant additions (MgO, CaO and SiO_2) on the microstructural features of alumina–zirconia composites.

2. Experimental procedure

2.1. Processing

Alumina powder (TM-DAR, Taimei Chem. Co. Ltd., Tokyo, Japan) and, respectively, 2.5, 10, 16 and 25 vol.% of zirconia powder (TZ0, Tosoh, Japan) were ball milled together in distilled water for 24 h, using alumina balls as grinding media. To avoid the use of a dispersant (hardly any of them are efficient for both alumina and zirconia, and the known versatile ones would possibly induce contamination of the slurries), electrostatic dispersion was chosen. The pH of the slurries was kept in the 3–4 range with the addition of HNO_3, where the ζ-potential is high for both alumina and zirconia, allowing optimum dispersion and agglomerate-free slurries.[9] Several amounts of calcium and magnesium were added to the slurries through the use of salts. $CaCl_2{\cdot}2H_2O$ was used at 0, 500, 3000 and 10,000 atomic ppm, and $MgCl_2{\cdot}6H_2O$ was used at 0, 200, and 5000 atomic ppm. SiO_2 was added as 40 nm colloidal particles (Ludox HS40) at 0, 500, 3000 and 10,000 atomic ppm ("ppm" relating to the number of doping cation as compared to the number of aluminum ions). Compositions were made with combinations of different amounts of dopants, sometimes using the three dopants (Ca, Si and Mg) in a same dispersion. Compositions and nomenclature are described as follows: zirconia amount/dopant amount and nature. For example:

10Z/200Mg stands for 10 vol.% of zirconia and 200 ppm of MgO.
2.5Z/500Ca/500Si/100Mg stands for 2.5 vol.% of zirconia, 500 ppm of CaO, 500 ppm of SiO_2 and 100 ppm of MgO.

Suspensions were de-aired in a vacuum desiccator and then poured into cylinder molds (10 mm height and diameter) consisting of a porous ceramic support (Al_2O_3–10 vol.% ZrO_2) and PVC "walls". The molds filled with the suspension were kept in humid atmosphere for 24 h before the samples were carefully removed.

After drying, for every composition, samples were sintered in air at different times and temperatures indicated in Table 1. The sintered specimens were machined with a resin-bonded diamond wheel (80 μm abrasives), then polished with diamond pastes down to 1 μm. To remove stresses induced by machining and polishing and also reveal the microstructure, all the samples were thermally etched for 30 min, 100 °C below the sintering temperature.

Table 1
Processing conditions of alumina-zirconia composites. All materials were sintered in air with heating ramp of 5 °C/min.

Doping	Sintering temperature (°C)	Dwell time (h)
Ca and/or Mg	1350	10
	1400	5
	1400	10
	1500	5
	1600	5
	1650	0
Si and/or Ca and/or Mg	1450	10
	1500	5
	1550	2
	1600	5
	1650	10

2.2. Characterization techniques

The final density of the specimens was determined by the Arthur's method, following ASTM C373-88 (Standard Test Method for Water Absorption, Bulk Density, Apparent Porosity, and Apparent Specific Gravity of Fired Whiteware Products).

Phase identification was performed on sintered and fractured surfaces using X-ray diffractometry (XRD, Brueker D8 Advance, Karlsruhe, Germany) with Cu Kα radiation. The integrated intensities of the diffraction peaks were obtained by stepwise counting the intensity using a step-size of 0.02° (2θ) and a counting time of 5 s per step. The tetragonal/monoclinic zirconia ratio was determined from the integrated intensity of the tetragonal (1 0 1) and t monoclinic (1 1 1) and ($\bar{1}$ 1 1) peaks, using the method proposed by Garvie and Nicholson[33] and modified by Toraya et al.,[34] as follows:

$$X_m = \frac{I_m(\bar{1}\ 1\ 1) + I_m(1\ 1\ 1)}{I_m(\bar{1}\ 1\ 1) + I_m(1\ 1\ 1) + I_q(1\ 0\ 1)} \quad (1a)$$

$$V_m = \frac{1.311 \times X_m}{1 + 0.311 \times X_m} \quad (1b)$$

where X_m (%) is the weight fraction and V_m (%) is the volume fraction of monoclinic phase (relative to the amount of zirconia only).

Microstructures were observed using a Zeiss Supra 55 VP scanning electron microscope, in vacuum and with an accelerating tension of 3 kV,

Average grain sizes and grain sizes distributions were estimated on SEM pictures using the linear intercept method. More than 100 grains and inclusions were counted, for each phase and each specimen in agreement with EN 623-3 and ASTM E 112.

3. Results

3.1. Ca or Mg doping

3.1.1. Density

The densities of the green powder compacts range from around 51% to 63.8% and depend on the composition. The more dopants are added, the lower the green density is. This is probably due to a destabilization of the slurry in the presence of the metallic salts. During sintering, rapid shrinkage begins at 1250 °C and the relative density reaches more than 99% around 1425 ± 5 °C for most samples. The sintering behavior of alumina is improved as the zirconia amount increases: shrinkage begins at lower temperature and shrinkage rate is higher. Differences in densification of samples with different amounts of dopants were observed, and are probably related to the differences in green density of the samples, due itself to a lower quality of the dispersion of the slurry in the presence of Mg and Ca. In any case, after sintering, samples of all compositions are dense (density higher than 97% of the theoretical density), except some of the ones sintered at lower temperature (1350 °C for 10 h) or for shorter time (1650 °C without annealing time).

3.1.2. Microstructure

SEM micrographs of polished and thermally etched samples are presented in Fig. 1 (in which zirconia and alumina are the bright and dark phases, respectively).

For the composites containing 2.5 vol.% of zirconia, few zirconia particles are embedded within the alumina grains (Fig. 1(c)). Moreover, with increasing temperature, more and more zirconia grains become relocated within the interior of alumina grains and possess an almost perfect spherical geometry with an average size of 100 nm. For the composites containing more than 2.5 vol.% of zirconia, the zirconia particles are mainly at the boundaries of the alumina matrix grains, and primarily located at 4-grain junctions, as illustrated in Fig. 1(a), (b) and (d). Zirconia particles located between alumina particles are sufficiently mobile during alumina grain growth to remain located at 4-joint junctions.

In Fig. 2, the zirconia and alumina grain sizes for every samples and every sintering temperatures disregarding the amount and nature of dopant used are reported. Increasing the temperature allows to increase grain size going from nano/nano composites (with 0.1–0.2 μm zirconia and 0.2–0.4 μm alumina: Fig. 1(a) and (d)) to micro-composites (0.6 μm zirconia and more than 1 μm alumina: Fig. 1(b)).

Increasing the amount of zirconia increases the zirconia grain size and decreases the alumina grain size as shown in Fig. 3, in agreement with Lange observations[35]: this is due to the dragging force exerted by zirconia grains to limit alumina matrix grains growth.

3.1.3. Dopants impact

Fig. 4(a) presents the evolution of alumina grain size with respect to the dopants and thermal treatments. At 1500 °C and below, considering the overlapping error bars, doping with Ca or Mg has almost no effect on alumina grain size: the observed changes are not statistically relevant. Neither calcium nor magnesium seems to influence the alumina grain size, whatever the thermal treatment. At 1600 °C and 1650 °C, it seems that Ca doping increases the alumina grain size, and that Mg-doping decreases it. However, even at these temperatures and for high Ca content, increasing the amount of zirconia still significantly decreases the alumina grain size, the effect of zirconia overcomes most of the effects dopants could have had. This

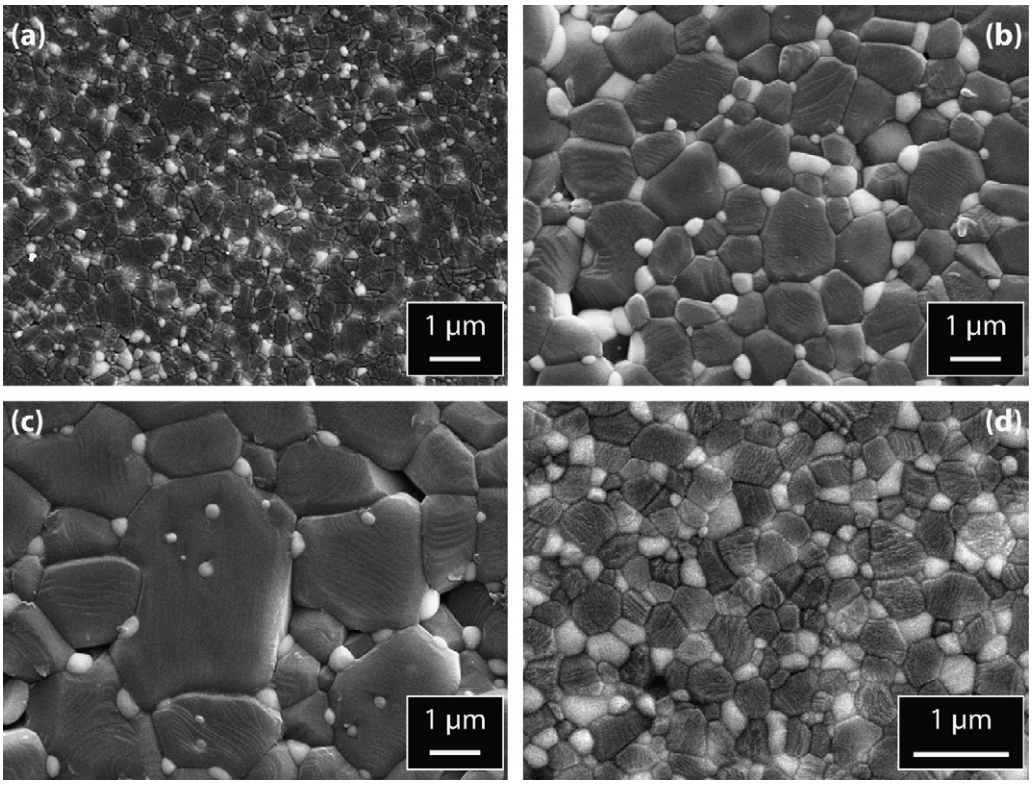

Fig. 1. SEM images of sintered samples: (a) 16Z/3000Ca, 1350 °C 10 h; (b) 10Z/5000Mg, 1650 °C 0 h; (c) 2.5Z/500Ca, 1650 °C 0 h; 25Z/200Mg, 1400 °C 10 h.

has been observed for every amount of zirconia whatever the quantity of dopant used (Fig. 4(b)).

3.1.4. Zirconia phase distribution

Fig. 5 presents the evolution of the monoclinic ratio of zirconia after sintering (monoclinic zirconia amount divided by total amount of zirconia). For a given zirconia grain size the monoclinic zirconia content increases with the total zirconia amount. One can notice that for low amount of zirconia (2.5 vol.%), all samples present a low monoclinic content (below 20 vol.%) and fine zirconia grains with a size comprise between 0.1 and

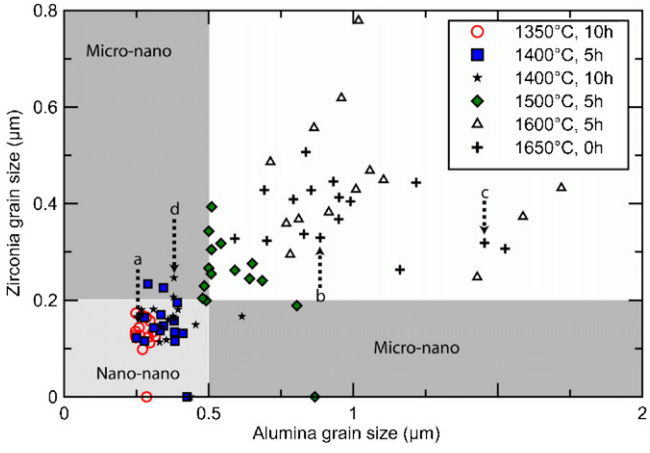

Fig. 2. Zirconia grain size as a function of alumina grain size in undoped and Ca- and Mg-doped composites. (a), (b), (c) and (d) are the reported SEM pictures of Fig. 1.

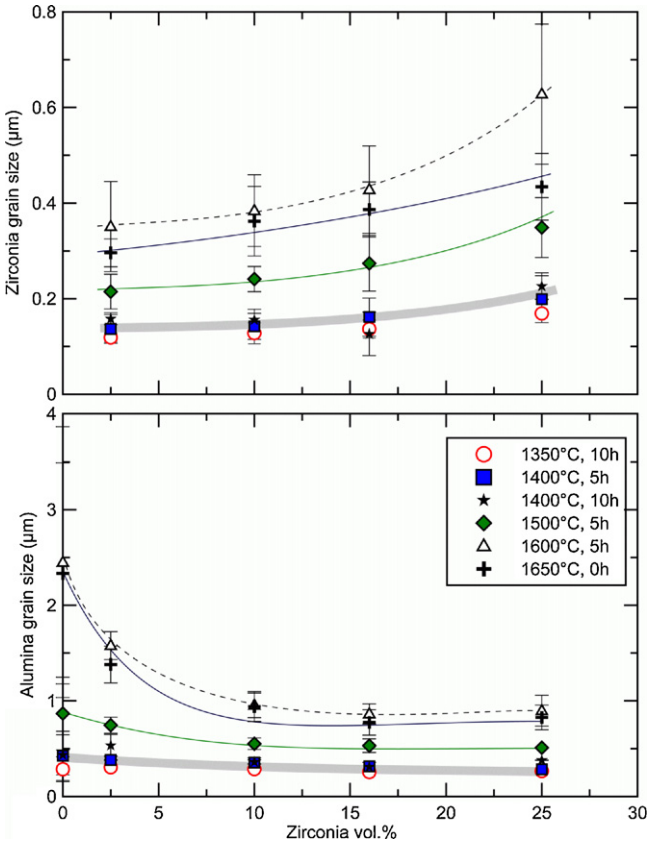

Fig. 3. Zirconia and alumina grain size as a function of the zirconia amount, for different thermal treatments.

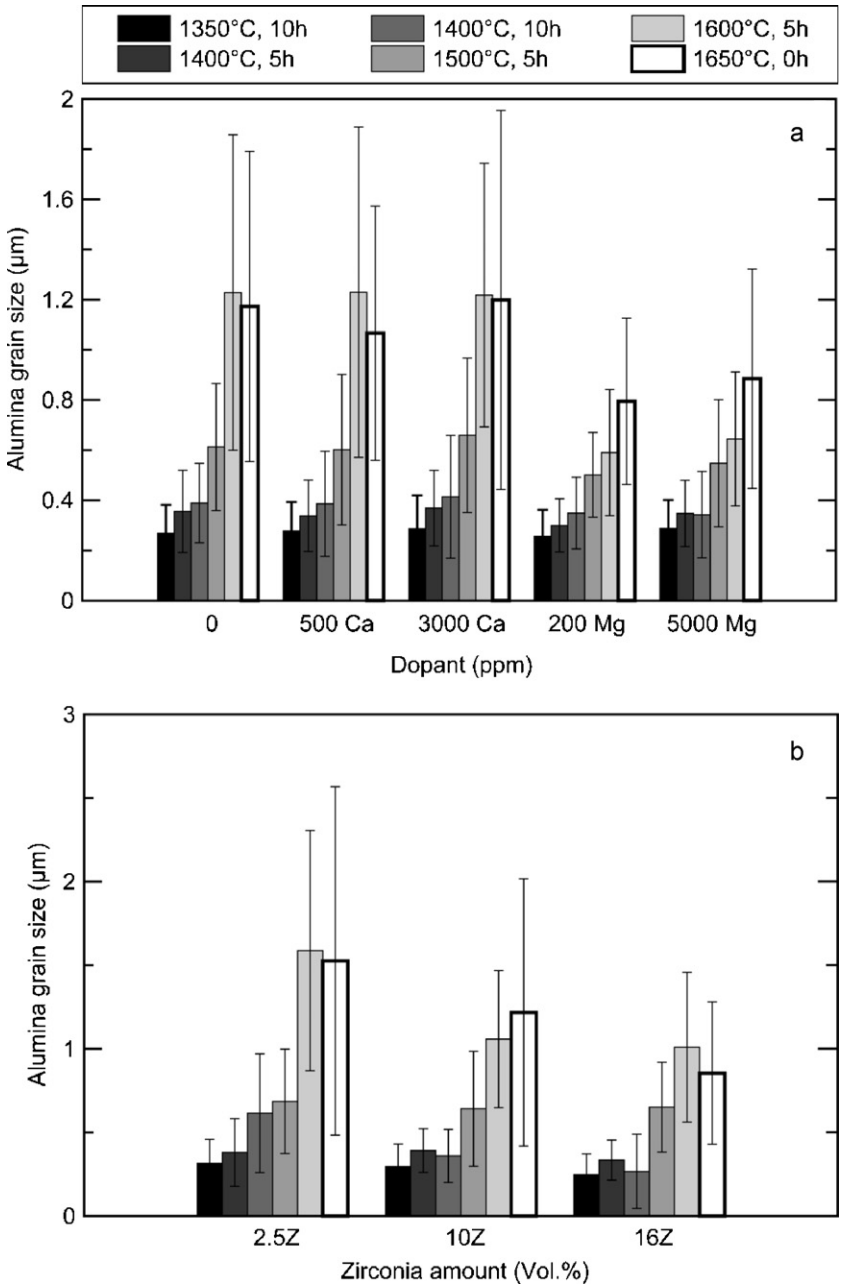

Fig. 4. Alumina grain size as a function of: (a) the dopant amount and nature for a composite containing 10 vol.% of zirconia and (b) the amount of zirconia and the thermal treatment in a composite with 3000 ppm Ca.

0.45 μm. This is verified for every temperature. On the contrary, every samples containing 25 vol.% whatever the sintering temperature used, show a high amount of monoclinic phase (V_m beyond 80%) and zirconia grains sizes spreading from 0.2 to 0.8 μm. For zirconia amounts around 10 and 16 vol.%, the monoclinic content increases with increasing sintering temperature, probably as a result of the increase of zirconia grain size and associated change in internal stresses. Moreover, for high sintering temperature around 1600–1650 °C, whatever the amount of zirconia (except for amount below 2.5 vol.%), a large part of zirconia grains transforms spontaneously from the tetragonal to the monoclinic phase during cooling after sintering.

3.2. *Effect of SiO_2 addition*

Intragranular zirconia grains have only been obtained with small additions of zirconia as shown before. Consequently in the will to elaborate micro/nano composites with a large number of intragranular zirconia particles, composites with 2.5 vol.% of zirconia sintered at different temperatures will be used as the base material. Many authors support the hypothesis that only the dual presence of silica and calcium leads to AGG.[36] Samples were consequently obtained with the additions of silica alone (2.5Z/0Ca/500Si/0Mg and 2.5Z/0Ca/3000Si/0Mg), and then with the addition

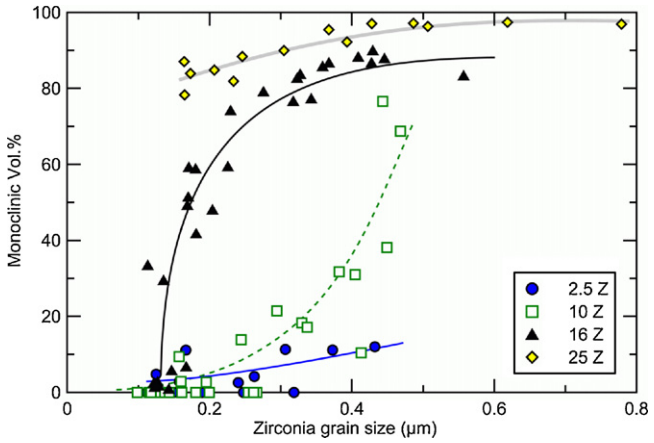

Fig. 5. Influence of the zirconia amount on the monoclinic phase evolution.

of silica and calcium (such as 2.5Z/500Ca/500Si/0Mg) or with the addition of silica, calcium and magnesium (like 2.5Z/500Ca/500Si/500Mg).

3.2.1. Density

The green density of samples ranges from 59% to 64% with an average around 61.5%. All sintered samples possess a density above 97%. Some sample sintered at 1650 °C with an annealing time of 10 h show a lower density that could be due to de-sintering phenomenon. It is important to notice that the more silica is added, the less dense sintered samples are.

3.2.2. Microstructures

With an amount of 2.5% of zirconia and the use of silica alone, for sintering temperatures between 1450 and 1650 °C, Fig. 6 shows that only few intragranular zirconia grains are obtained. The absence of zirconia agglomerates indicates a homogeneous distribution of both phases in the composite. Alumina grains present a relatively large grain size distribution (0.1–20 μm depending of the sintering temperature) and many grains are tabular or elongated. Zirconia particles are smaller (0.18–2 μm for intergranular and 0.1–0.5 μm for intragranular zirconia grain) and are isolated at GB between larger alumina grains or inside alumina grains. Intragranular zirconia particles show an almost perfect spherical shape with a median grain size of 220 nm. X-ray diffraction experiments hint that these zirconia particles are mainly tetragonal, although the amount of monoclinic phase slightly increases with sintering temperature.

De-sintering phenomenon may be observed in samples sintered above 1600 °C with the apparition of intergranular porosity and a slight decrease in their density compare to samples sintered around 1400–1500 °C.

Co-doping with silica and calcium leads to micro/nano composites presented in Fig. 7 with a high proportion of intragranular zirconia particles homogeneously distributed inside the alumina grains. There is almost no intragranular porosity in alumina grains. However, a high number of intergranular porosities is observed, which do not seem to critically decrease the sintered density.

Below 1500 °C the alumina grain size ranges from 0.3 μm to 8 μm, with large, mostly facetted abnormal grains surrounded

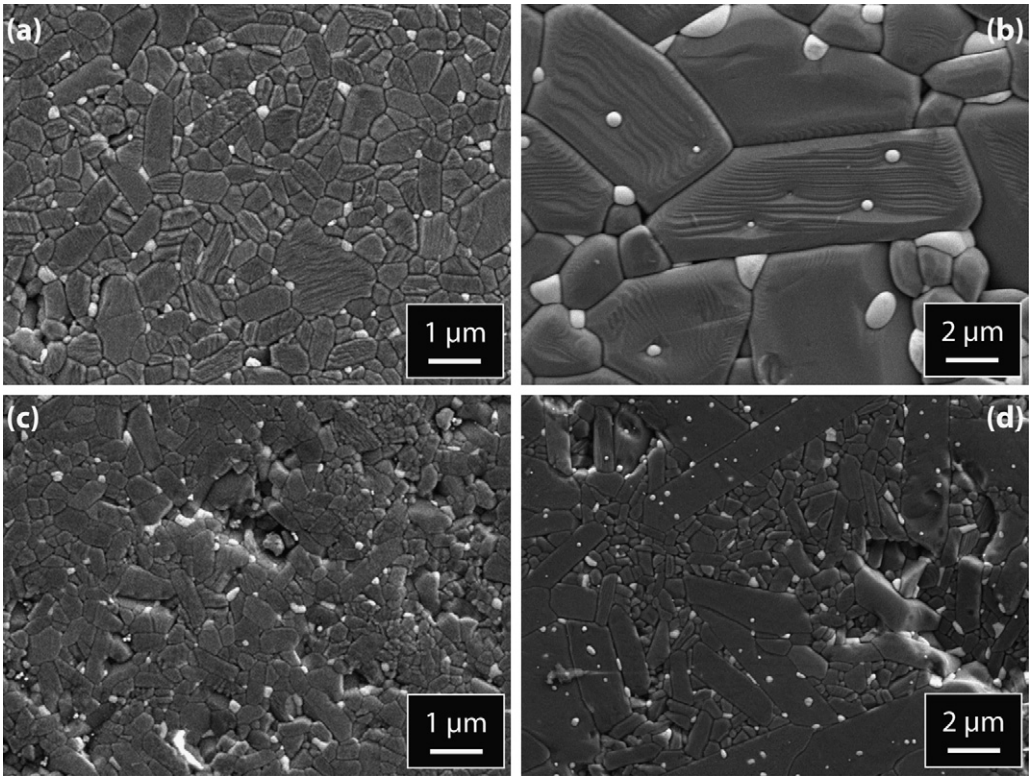

Fig. 6. SEM micrographs of Si-doped ZTA: (a) 1450 °C + 10 h, 2.5Z/0Ca/500Si/0 Mg; (b) 1650 °C + 10 h, 2.5Z/0Ca/500Si/0 Mg; (c) 1450 + 10 h, 2.5Z/0Ca/3000Si/0 Mg; (d) 1550 °C + 2 h, 2.5Z/0Ca/3000Si/0 Mg.

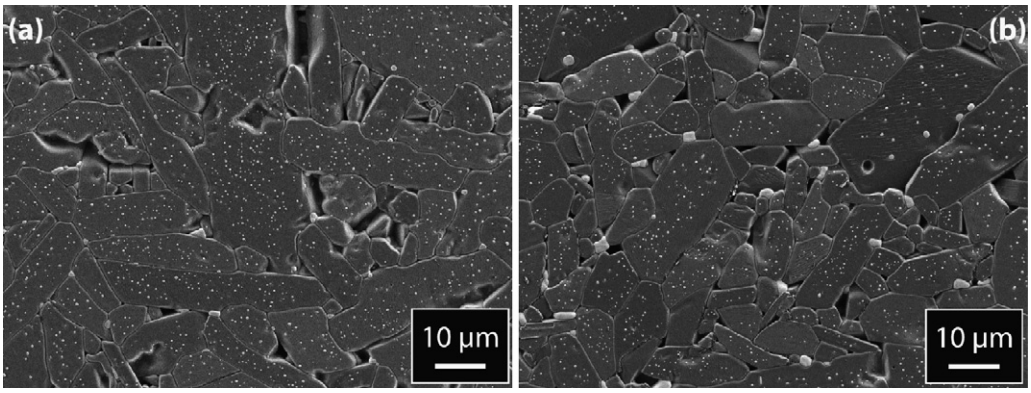

Fig. 7. SEM micrographs of Ca + Si co-doped ZTA: (a) 1600 °C + 5 h, 2.5Z/3000Ca/500Si/0 Mg and (b) 1600 °C + 5 h, 2.5Z/10,000Ca/10,000Si/0 Mg.

by cluster of small grains. These clusters are composed of fine alumina grains both elongated and isotropic. Grain boundaries between the fine matrix grains appear to be slightly curved. Some of the largest alumina abnormal grains are lath-shaped, elongated in the direction probably parallel to their basal plane (0 0 0 1). Those grains often present straight boundary segments in contact with smaller grains along the elongated section.

Above 1600 °C, most of alumina grains are large (from 3 to 20 μm with an average size around 8 μm and aspect ratio generally between 2 and 5). The grain growth behavior of highly doped samples leads to structures with only few intergranular zirconia grains located at multiple grain boundaries. Those grains possess spherical shapes with an average size around 1–2 μm. Most of the zirconia grains are located inside alumina grains and remain small (0.3 μm) and spherical. Samples with 10,000 ppm Ca additions contain traces of calcium hexaluminate (CA6), in proportions increasing with the sintering temperature.

Doping with silica can generate much faster grain growth than doping with calcium or magnesium alone: these highest alumina grain sizes obtained with Si- or Si + Ca-doping are, respectively, five and three times higher than the highest sizes measured for alumina and zirconia grain with Ca and/or Mg doping (without Si) (Fig. 8). However, low sintering temperatures generally allow maintaining rather small grain sizes (<0.8 μm for zirconia, and <2 μm for alumina).

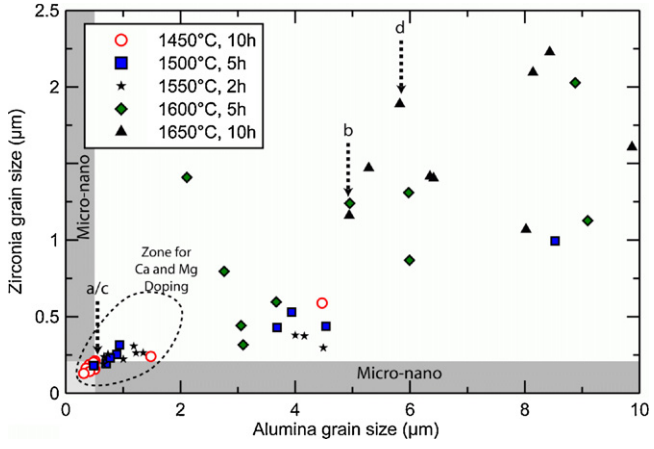

Fig. 8. Alumina average grain sizes as a function of zirconia average grain size in Si-doped composites. Microstructures of Fig. 8 are reported (a, b, c, and d) as well as the area representing the Ca- and Mg-doped composites (dotted area).

Fig. 9 represents the proportion of intragranular zirconia grains (versus total number of zirconia grains) for all compositions. For low dopant contents, sintering temperatures above 1550 °C are needed to maximize the ratio of intragranular zirconia grains, whereas for high dopant contents (higher than 0Ca/3000Si and 3000Ca/500Si), sintering temperatures of 1500 °C are sufficient. However, in the presence of magnesium and below 1500 °C, zirconia grains remain intergranular even with high amounts of silica.

Fig. 10 represents the grain size distribution of alumina, intergranular zirconia (Zinter) and intragranular zirconia (Zintra), for the following compositions: 2.5 vol.% of zirconia and 500 ppm of silica (2.5Z/Si500). At low temperature, for example 1450 °C with an annealing time of 10 h, very few intragranular zirconia grains are observed. Intergranular and intragranular zirconia grain size distributions remain narrow with sizes ranging from under 0.1 to 0.4 μm for both kinds of zirconia grains, even though intra grains are generally smaller. Alumina grains are still small considering the original powder size (150 nm) with sizes ranging from 0.1 to 2 μm, and an average grain size around 0.5 μm. As the sintering temperature increases, the three grain sizes distributions progressively widen while the average grain sizes increase, and the intergranular zirconia grain size increases much faster with temperature than intragranular zirconia grain size. At 1650 °C, intragranular zirconia grains are observed with sizes ranging from 0.2 to 2 μm with an average size around 0.5 μm while intergranular zirconia grains are larger (ranging from 0.3 to 3 μm with an average size around 2 μm). Alumina is growing faster and the distribution width is ten times its value at low temperature. Alumina grains range from 2 to 25 μm with an average size around 5 μm. The three kinds of grains are clearly separated in sizes. This evolution of the grain sizes distribution, presented here on one composition, is relevant for every composition.

3.2.3. Zirconia phase distribution

Samples containing silica present a progressive increase of monoclinic content with sintering temperature, however, the monoclinic fraction always remain low (below 20%). For low dopant contents and at low temperature (below 1550 °C), the

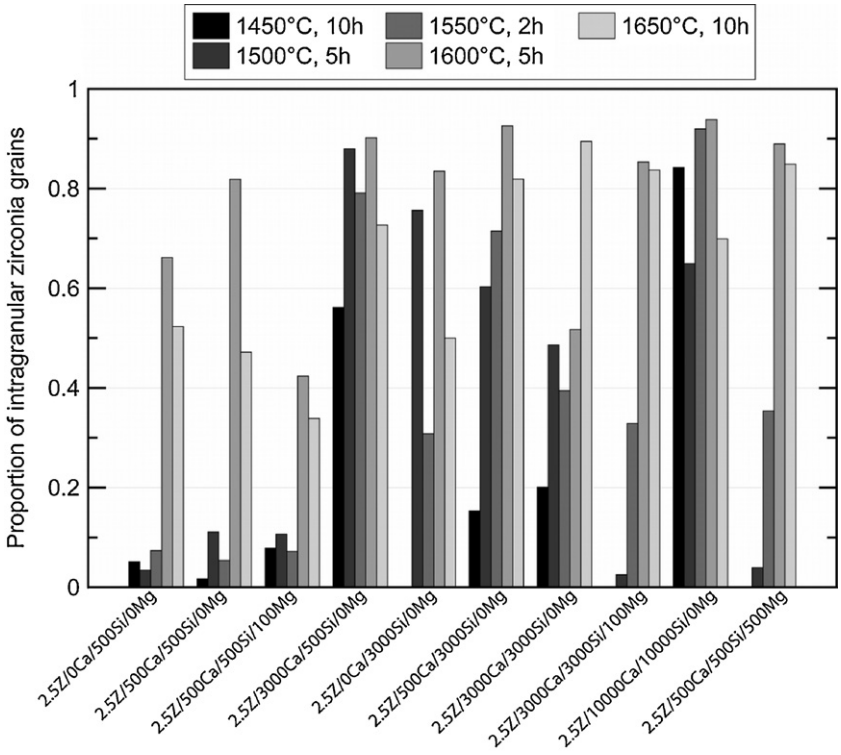

Fig. 9. Proportion of intragranular zirconia grains a function of the composition in Si-doped ZTA composites.

monoclinic fraction even stays under 10%. Despite the fact that the majority of zirconia particles are quite below the critical size for phase transformation, intergranular particles present large sizes compared to intragranular ones and consequently are more likely to be monoclinic (Fig. 11).

4. Discussion

On first approximation the microstructures obtained here result from a balance between the pinning effect of zirconia particles and the mobility of alumina grain boundaries. Co-doping with Ca and Si results in highly mobile grain boundaries, that overcome the pinning effect resulting in intragranular zirconia particles trapped inside large alumina grains. All other dopings result in lower mobility of the grain boundaries, thus mainly in intergranular zirconia particles.

Considering the types and amounts of dopants used in this study (Mg, Ca and Si), it can be assumed that most doping atoms should concentrate at the grain boundaries and may form an intergranular phase,[20,37] thus affecting grain boundaries mobility. These chemical elements are indeed reported to affect the sintering behavior and grain shape of alumina ceramics: MgO is known to improve alumina densification and reduce its grain size, whereas CaO and SiO_2 impurities lead to abnormal grain growth.

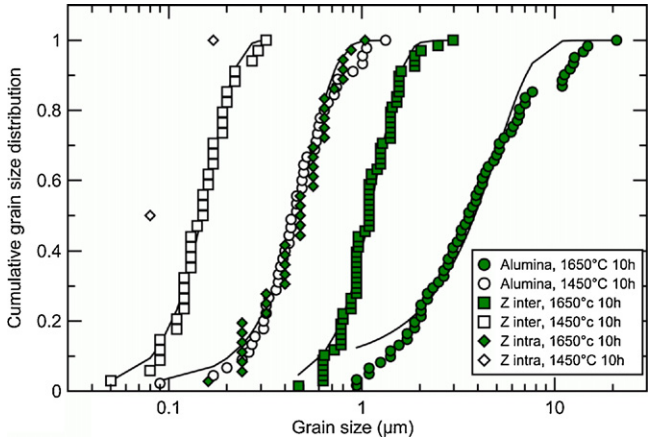

Fig. 10. Cumulative grain size distributions for 2.5Z/500Si sintered at 1450 °C + 10 h and 1650 °C + 10 h. The continuous lines represent fits with normal distributions.

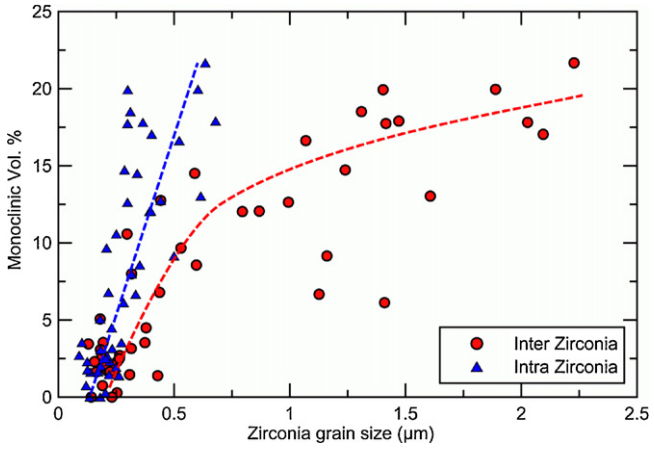

Fig. 11. Monoclinic content versus zirconia average grain size (for intragranular and intergranular zirconia grains).

One unexpected result of this study is the fact that doping ZTA with a single one of these elements has almost no influence on the final microstructure. This is especially true for sintering temperatures lower than 1500 °C: microstructural observations of Ca or Mg or Si single-doped composites indicate that only increasing amounts of zirconia provide a significant decrease in alumina grain size. Higher temperatures (above 1600 °C) and low amount of zirconia (2.5 vol.%) are needed to increase alumina grain size with calcium or silica doping. On the one hand, this indicates that the pinning effect of zirconia particles is much more efficient to reduce the grain size than doping with MgO, while one could have expected a "symbiotic" action of these two grain-size reducers. On the other hand, this indirectly shows that the increase in grain size mobility brought by Ca and Si single-doping strongly depends on temperature: at low temperature, it is not sufficient to overcome the pinning effect of zirconia particles.

On the contrary, doping with combinations of Si and Ca is quite effective to trigger fast growth of alumina grains. Once again, the effect is related to temperature, but sintering temperatures as low as 1500 °C are sufficient to obtain high mobility grain boundaries. The effect is also related to the quantity of dopants: no clear effect is obtained for global Si + Ca doping lower than 3500 ppm. This is a quite high level as compared to the amount of impurities reported in the literature to provoke abnormal grain growth.[29,30,38] It could be related to the starting alumina grain size: the TM DAR powder used here has an average particle size of 150 nm, which is much lower than most values in the literature (350 nm[39]). However, since the ratio amount of dopant/specific surface area is around 250 ppm/($m^2\ g^{-1}$) here versus 20 in the literature,[40] the smaller particle size cannot be the only explanation. This hints that the pinning effect of zirconia grains implies the use of high amounts of dopants to allow for fast alumina grain growth.

Generally speaking, all these results are coherent with the complexions theory.[20,21] Alumina is known to display several complexions, depending on sintering temperature and chemistry. AGG would result from the coexistence of two or more complexions around a single grain. This would explain why an additive that stabilizes one single complexion will promote NGG, MgO is known indeed to stabilize low mobility, highly ordered complexions. On the other hand additives that stabilize multiple complexions with different mobilities at a single temperature, such as Si and Ca, will enhance AGG, and in our case allow fast grain boundaries movements and the entrapment of zirconia particles (Fig. 12(a)). Thus adding both Si, Ca and Mg result in an equilibrium in which AGG can be controlled and the average alumina grain size decreased, as it is illustrated in Fig. 12(c). However, increasing grain boundary mobility thanks to disordered complexions is not without drawbacks: a disordered complexion is rather like a glassy phase that may not be wanted in alumina because it could decrease its mechanical properties and chemical inertness. The presence of important quantities of this glassy phase is illustrated in Fig. 12(d), that shows an almost continuous phase on the grain boundary, attributed to the squeezing of the glassy phase in excess from the grain boundaries during the thermal etching prior SEM observation.

To complete this explanation, however, one factor not yet considered is the interfacial energy between the grain boundary phases or complexions and the zirconia particles: it is possible that high interfacial energy leads to partial or no wetting of the zirconia particles by the grain boundary phase, reinforcing their pinning effect. On the other hand, low interfacial energy may result in complete wetting of the zirconia particles by the grain boundary phase, neutralizing the pinning effect by providing a fast diffusion path around the zirconia particles.

The same balance between grain boundaries mobility, pinning effect of the zirconia particles and zirconia/grain boundary phase interfacial energy could explain both sintering behavior (faster densification of the composites) and evolution of the zirconia grain size. Due to their small size and to the efficient electrostatic dispersion, zirconia particles are homogeneously distributed in the bulk. They can then pin alumina grain boundaries, resulting in highly curved boundaries, and effectively impairing grain growth and thus favoring densification during the sintering thermal treatment (such a curved grain boundary is shown in Fig. 12(b)). At higher temperature, if the alumina grain boundaries mobility is high enough (as it is the case for Si + Ca co-doping) such zirconia grains could be swallowed by the growing alumina grain, leading to intragranular zirconia particles and allowing abnormal grain growth. Once inside the alumina grains, diffusion from and to the zirconia grains becomes difficult (no easy path for Zr ions through alumina grains), keeping the intragranular zirconia grains rather small. On the contrary, if the alumina grain boundaries mobility is not very high (in Ca or Mg singly-doped materials or for materials sintered at lower temperatures), the pinning effect of zirconia particles endures, and zirconia grains grow themselves larger as they remain at the grain boundary and the diffusion between them is relatively easy.

Another important feature in ZTA is the state of the zirconia grains: monoclinic or tetragonal. Indeed, this will directly influence the mechanical properties, through different toughening mechanisms. Generally, high monoclinic contents are related to large zirconia grain sizes, and can result in toughening by microcracking. Such a behavior is expected in samples sintered at high temperature, with Ca or Mg for only dopants. Smaller zirconia grains are most often tetragonal, thus susceptible to tetragonal to monoclinic transformation and to give rise to phase transformation toughening. The same Ca or Mg singly-doped composites, but sintered at lower temperature, should present this kind of toughening mechanism. Even smaller, intragranular zirconia grains are believed to lead to very high residual stresses and stress-related toughening mechanism. This is what is expected from the composites co-doped with Si and Ca, in which many or most zirconia grains are intragranular.

Another important finding of this article is the fact that the critical zirconia grain size for spontaneous tetragonal to monoclinic transformation upon cooling after sintering is strongly dependent on the amount of zirconia in the composite. Two complementary explanations might be considered. First, as the

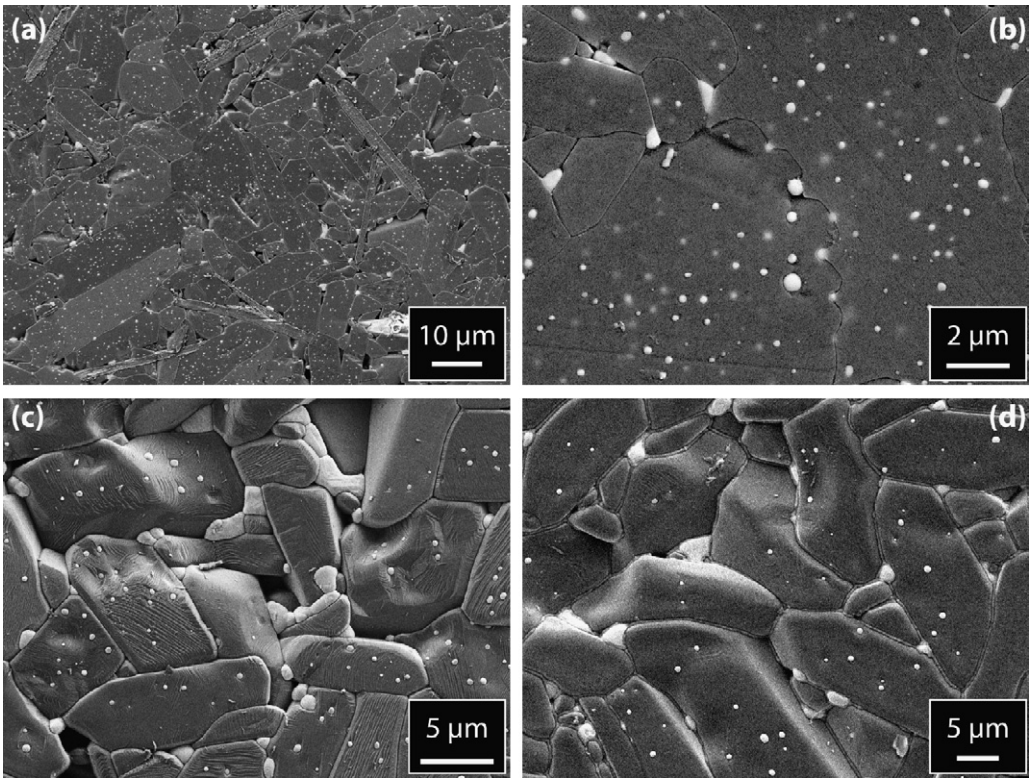

Fig. 12. SEM micrographs of Si–Ca–Mg-co-doped ZTA samples. (a) 1500 °C + 5 h, 2.5Z/10,000Ca/10,000Si; (b) 1600 °C + 5 h, 2.5Z/3000Ca/3000Si/100Mg; (c) 1600 °C + 5 h, 2.5Z/500Ca/500Si/500Mg; and (d) 1650 °C + 10 h, 2.5Z/3000Ca/500Si.

amount of zirconia increases, the overall stiffness of the composite decreases and the stabilization by alumina matrix is less efficient. Second, increasing the amount of zirconia also increases the internal stresses that could trigger the *t–m* transformation upon cooling after sintering. It has been proven that increasing the zirconia amount up to 10 vol.% raises the critical size for zirconia transformation until 566 nm, because the residual stresses prevails. But beyond this content the critical size decreases due to the interaction between grains that cannot be neglected any longer. Thus the matrix constraint and the residual stresses due to the thermal mismatch increase the probability of *t*-zirconia transformation generating microcracks and the alumina matrix weakness.[32]

5. Conclusion

Controlling ZTA microstructures has proven to be very delicate. Despite the use of different types and amount of dopants, many microstructures remain similar. The use of calcium associated or not with magnesium seems useless as compared to the predominant influence of the zirconia content. On the other side, Si/Ca co-doped ZTA composites with small amount of zirconia (2.5 vol.%) leads to almost homogeneous micro/nano composites with intragranular zirconia particles at high temperatures (above 1500 °C). The effects of the dopants and the sintering cycles are related to a balance between grain boundary mobility (increased by Si and Ca doping and high temperature) and pinning by zirconia particles (more effective for high zirconia contents).

Acknowledgment

This work has been supported by ANR (AgenceNationale de la Recherche) under Grant number MAPR07-0014.

References

1. Chevalier J, Taddei P, Gremillard L, Deville S, Fantozzi G, Bartolomé JF, et al. Reliability assessment in advanced nanocomposite materials for orthopaedic applications. *Journal of the Mechanical Behavior of Biomedical Materials* 2011;**4**:303–14, doi:10.1016/j.jmbbm.2010.10.010.
2. Chevalier J, Gremillard L. Ceramics for medical applications: a picture for the next 20 years. *Journal of the European Ceramic Society* 2009;**29**(7):1245–55.
3. Kuntz M, Shneider N, Heros R. Controlled zirconia phase transformation in BIOLOX® delta—a feature of safety. In: *Bioceramics and alternative bearings in joint arthroplasty, ceramic in orthopaedics*. 2007. p. 4.
4. Kobayashi K, Kuwajima H, Masaki T. Phase change and mechanical properties of ZrO_2–Y_2O_3 solid electrolyte after ageing. *Solid State Ionics* 1981;**3–4**:489–93.
5. Chevalier J, Grandjean S, Kuntz M, Pezzotti G. On the kinetics and impact of tetragonal to monoclinic transformation in an alumina/zirconia composite for arthroplasty applications. *Biomaterials* 2009;**30**(29):5279–82.
6. Pezzotti G, Yamada K, Sakakura S, Pitto RP. Raman spectroscopic analysis of advanced ceramic composite for hip prosthesis. *Journal of American Ceramic Society* 2008;**91**(4):1199–206.
7. Deville S, Chevalier J, Fantozzi G, Bartolomé JF, Requena J, Moya JS, et al. Low-temperature ageing of zirconia-toughened alumina ceramics and its implication in biomedical implants. *Journal of the European Ceramic Society* 2003;**23**(15):2975–82.
8. Deville S, Chevalier J, Dauvergne C, Fantozzi G, Bartolomé JF, Moya JS, et al. Microstructural investigation of the aging behavior of (3Y-TZP)–Al_2O_3 composites. *Journal of American Ceramic Society* 2005;**88**(5):1273–80.

9. Gutknecht D, Chevalier J, Garnier V, Fantozzi G. Key role of processing to avoid low temperature ageing in alumina zirconia composites for orthopaedic application. *Journal of the European Ceramic Society* 2007;**27**(2–3):1547–52.
10. Maneshian M, Banerjee M. Effect of sintering on structure and mechanical properties of alumina–15 vol% zirconia nanocomposites compacts. *Journal of Alloys and Compounds* 2010;**493**(1–2):613–8.
11. Prabhu GB, Bourell DL. Synthesis and sintering characteristics of zirconia and zirconia–alumina nanocomposites. *Nanostructured Materials* 1995;**6**(1–4):361–4.
12. Gutknecht D. *Elaboration et caractérisation de micro et nanocomposites alumine–zircone pour application orthopédique*. Lyon: INSA; 2006.
13. Bartolomé JF, De Aza AH, Martín A, Pastor JY, Llorca J, Torrecillas R, et al. Alumina/zirconia micro/nanocomposites: a new material for biomedical applications with superior sliding wear resistance. *Journal of the American Ceramic Society* 2007;**90**(10):3177–84.
14. Niihara K. New design concept of structural ceramics–ceramic nanocomposites. *Journal of the Ceramic Society of Japan* 1991;**99**:974–82.
15. Dillon SJ, Harmer MP. Intrinsic grain boundary mobility in alumina. *Journal of the American Ceramic Society* 2006;**89**(12):3885–7.
16. Bae IJ, Baik SG. Abnormal grain growth of alumina. *Journal of American Ceramic Society* 1997;**80**(5):1149–56.
17. Rollett A, Srolovitz D, Anderson M. Simulation and theory of abnormal grain growth: anisotropic grain boundary energies and mobilities. *Acta Metallurgica* 1989;**37**(4):1227–40.
18. Prabhu GB, Bourell DL. Abnormal grain growth in alumina–zirconia nanocomposites. *Nanostructured Materials* 1995;**5**(6):727–32.
19. Dillon SJ, Harmer MP. Diffusion controlled abnormal grain growth in ceramics. In: *Materials science forum*. Island: Jeju; 2007. p. 1227–36.
20. Dillon SJ, Tang M, Carter WC, Harmer MP. Complexion: a new concept for kinetic engineering in materials science. *Acta Materialia* 2007;**55**(18):6208–18.
21. Dillon SJ, Harmer MP. Demystifying the role of sintering additives with "complexion". *Journal of the European Ceramic Society* 2008;**28**(7):1485–93.
22. Shaw NJ, Brook RJ. Structure and grain coarsening during the sintering of alumina. *Journal of American Ceramic Society* 1986;**69**(2):3.
23. Bae SI, Baik S. Critical concentration of MgO for the prevention of abnormal grain growth in alumina. *Journal of American Ceramic Society* 1994;**77**(10):2404–99.
24. Berry KA, Harmer MP. Effect of MgO solute on microstructure development in Al_2O_3. *Journal of American Ceramic Society* 1986;**69**(2):6.
25. Ganesh I, Ferreira JMF. Synthesis and characterization of $MgAl_2O_4$–ZrO_2 composites. *Ceramics International* 2009;**35**(1):259–64.
26. Hossein A. *Elaboration et caractérisation de composites duplex "composites laminaires tri-couches à base d'alumine"*; 1997.
27. Park CW, Yoon DY. Effects of SiO_2, CaO_2, and MgO additions on the grain growth of alumina. *Journal of American Ceramic Society* 2000;**83**(10):2605–9.
28. Gavrilov.K L, Bennison.S J, Mikeska.K R, Chabala.J M, Levi-Setti R. Silica and magnesia dopant distributions in alumina by high-resolution scanning secondary ion mass spectroscopy. *Journal of American Ceramic Society* 1999;**82**(4):7.
29. Louet N. *Influence du dopage à la silice ou à l'oxyde de calcium sur le frittage et sur l'évolution microstructurale d'une alumine-alpha ultra pure*. Lyon: Institut Nationale des Sciences Appliquées de Lyon; 2003.
30. Dillon SJ, Harmer MP. Relating grain-boundary complexion to grain-boundary kinetics I: calcia-doped alumina. *Journal of the American Ceramic Society* 2008;**91**(7):2304–13.
31. Yoshida H, Hashimoto S, Yamamoto T. Dopant effect on grain boundary diffusivity in polycrystalline alumina. *Acta Materialia* 2005;**53**(2):433–40.
32. Naglieri V. Alumina–zirconia composites: elaboration and characterization, in view of the orthopaedic application. *Torino* 2010.
33. Garvie RC, Nicholson PS. Phase analysis in zirconia systems. *Journal of the American Ceramic Society* 1972;**55**(6):303–5.
34. Toraya H, Yoshimura M, Somiya S. Calibration curve for quantitative analysis of the monoclinic-tetragonal ZrO_2 system by X-ray diffraction. *Journal of the American Ceramic Society* 1984;**67**(6): C-119–21.
35. Lange FF. Transformation toughening – part 4 fabrication, fracture toughness and strength of Al_2O_3–ZrO_2 composites. *Journal of Materials Science* 1982;**17**(1):247–54.
36. Song H, Coble RL. Morphology of platelike abnormal grains in liquid-phase-sintered alumina. *Journal of the American Ceramic Society* 1990;**73**(7):2086–90.
37. Dillon SJ, Miller H, Harmer MP, Rohrer GS. Grain boundary plane distributions in aluminas evolving by normal and abnormal grain growth and displaying different complexions. *International Journal of Materials Research* 2010;**101**(1):50–6.
38. Dillon SJ, Harmer MP. Relating grain-boundary complexion to grain-boundary kinetics II: silica-doped alumina. *Journal of the American Ceramic Society* 2008;**91**(7):2314–20.
39. Palmero P, Naglieri V, Chevalier J, fantozzi G, Montanaro L. Alumina-based nanocomposites obtained by doping with inorganic salt solutions: application to immiscible and reactive systems. *Journal of the European Ceramic Society* 2009;**29**:7.
40. Bae SI, Baik S. Determination of critical concentrations of silica and/or calcia for abnormal grain growth in alumina. *Journal of American Ceramic Society* 1993;**76**(4):2.